

UC Irvine

UC Irvine Previously Published Works

Title

Persistent El Niño driven shifts in marine cyanobacteria populations

Permalink

<https://escholarship.org/uc/item/79w86965>

Journal

PLOS ONE, 15(9)

ISSN

1932-6203

Authors

Larkin, Alyse A

Moreno, Allison R

Fagan, Adam J

et al.

Publication Date

2020

DOI

10.1371/journal.pone.0238405

Copyright Information

This work is made available under the terms of a Creative Commons Attribution License, available at <https://creativecommons.org/licenses/by/4.0/>

Peer reviewed

RESEARCH ARTICLE

Persistent El Niño driven shifts in marine cyanobacteria populations

Alyse A. Larkin¹, Allison R. Moreno², Adam J. Fagan¹, Alyssa Fowlds¹, Alani Ruiz¹, Adam C. Martiny^{1,2*}

1 Department of Earth System Science, University of California at Irvine, Irvine, California, United States of America, **2** Department of Ecology and Evolution, University of California at Irvine, Irvine, California, United States of America

* amartiny@uci.edu



OPEN ACCESS

Citation: Larkin AA, Moreno AR, Fagan AJ, Fowlds A, Ruiz A, Martiny AC (2020) Persistent El Niño driven shifts in marine cyanobacteria populations. *PLoS ONE* 15(9): e0238405. <https://doi.org/10.1371/journal.pone.0238405>

Editor: Chih-hao Hsieh, National Taiwan University, TAIWAN

Received: April 10, 2020

Accepted: August 15, 2020

Published: September 16, 2020

Copyright: © 2020 Larkin et al. This is an open access article distributed under the terms of the [Creative Commons Attribution License](https://creativecommons.org/licenses/by/4.0/), which permits unrestricted use, distribution, and reproduction in any medium, provided the original author and source are credited.

Data Availability Statement: All DNA sequence files are available from the NCBI Sequence Read Archive database (accession number PRJNA624320). All environmental data is in the process of being amended to project web page in the BCO-DMO database (DOI:[10.26008/1912/bco-dmo.564351.2](https://doi.org/10.26008/1912/bco-dmo.564351.2)).

Funding: Financial support for this work was provided by the UCI Undergraduate Research Opportunities Program (to AJF and AF), NSF Graduate Research Fellowship Program and UCI Chancellor's Club Fellowship (to ARM), and NSF

Abstract

In the California Current Ecosystem, El Niño acts as a natural phenomenon that is partially representative of climate change impacts on marine bacteria at timescales relevant to microbial communities. Between 2014–2016, the North Pacific warm anomaly (a.k.a., the “blob”) and an El Niño event resulted in prolonged ocean warming in the Southern California Bight (SCB). To determine whether this “marine heatwave” resulted in shifts in microbial populations, we sequenced the *rpoC1* gene from the biogeochemically important picocyanobacteria *Prochlorococcus* and *Synechococcus* at 434 time points from 2009–2018 in the MICRO time series at Newport Beach, CA. Across the time series, we observed an increase in the abundance of *Prochlorococcus* relative to *Synechococcus* as well as elevated frequencies of ecotypes commonly associated with low-nutrient and high-temperature conditions. The relationships between environmental and ecotype trends appeared to operate on differing temporal scales. In contrast to ecotype trends, most microdiverse populations were static and possibly reflect local habitat conditions. The only exceptions were microdiversity from *Prochlorococcus* HLI and *Synechococcus* Clade II that shifted in response to the 2015 El Niño event. Overall, *Prochlorococcus* and *Synechococcus* populations did not return to their pre-heatwave composition by the end of this study. This research demonstrates that extended warming in the SCB can result in persistent changes in key microbial populations.

Introduction

Ocean warming may be driving an areal increase of the globe's oligotrophic gyres through increased stratification and weaker nutrient entrainment [1, 2]. Marine bacterioplankton may be sensitive to this global ocean change. To date, ocean time series efforts have shown that marine bacteria are highly responsive to seasonal environmental cycles [3–6] and display a slow decay in community similarity on an annual to multi-annual scales [7, 8]. Paleo-oceanographic evidence suggests that climatic tipping points can lead to relatively rapid shifts in plankton community composition, including cyanobacteria [9]. However, across systems,

Biological Oceanography (OCE-1848576 and OCE-1948842 to ACM). The funders had no role in study design, data collection and analysis, decision to publish, or preparation of the manuscript.

Competing interests: The authors have declared that no competing interests exist.

seasonal patterns in bacterial community composition have generally been resilient to discrete, or “pulse,” disturbances such as storms and short-term anthropogenic impacts [10–13]. Moreover, quantitative measurements of the response of marine bacteria to warming experiments *in situ* are rare [14], particularly in comparison to the range of warming experiments in soils and other ecosystems [15]. In contrast, a multitude of studies have shown that eukaryotic marine phytoplankton and zooplankton show significant changes in community structure in response to longer-term climatic warming oscillations on time scales from El Niño to the Atlantic Multidecadal Oscillation [16–18]. Thus, empirical observations of bacterioplankton responses to *in situ* ocean warming are both limited and critical for understanding how ocean ecosystems respond to climate change.

Given the rapid generation times of marine bacteria, El Niño is a natural laboratory that can be used to understand bacterioplankton responses to multiannual-scale ocean warming and climate change impacts in the North Pacific Ocean. From 2014 through 2016, the Warm Anomaly and a significant El Niño event resulted in a prolonged “marine heatwave” across the Eastern North Pacific Ocean [19, 20]. In the Southern California Bight (SCB), these events resulted in suppressed primary production but little to no change in C export [21, 22]. Stratification and lower nutrient supply led to reduced particulate organic matter concentrations with concurrent high carbon:phosphorus (C:P) and nitrogen:phosphorus (N:P) ratios [23]. Previous studies of plankton communities in the SCB revealed increasing cyanobacteria cell abundance [5]. In addition, zooplankton populations showed significant changes in composition at the species level [24], suggesting that warming has a significant effect on planktonic communities in this region. Prior to the 2014–16 events, an analysis of hydrographic data (1984–2012) from the California Cooperative Oceanic Fisheries Investigations (CalCOFI) program revealed declining inorganic N:P ratios at coastal locations in the SCB [25]. Based on these observations, we predicted that prolonged warming, decreased nutrient availability, and shifting N:P ratios due to the 2014–2016 climate anomalies would also result in a shift in marine cyanobacteria populations.

The highly abundant, widely distributed, and biogeochemically significant cyanobacteria *Prochlorococcus* and *Synechococcus* represent an important model system that can be used to determine the impact of changing environmental conditions on population-specific microbial diversity. Both genera are characterized by genomic traits associated with light, temperature, and nutrient optima that drive variable, clade-specific biogeographic patterns of abundance at high levels of phylogenetic similarity [26–30]. Thus, the phylogenetic diversity of these genera (i.e., ecotypes [31]) can be readily associated with subtle ocean changes due to our extensive knowledge of their respective trait distributions [32]. Previous time series studies of *Synechococcus* and *Prochlorococcus* have demonstrated stable interannual patterns of relative ecotype abundance as well as seasonal switching in either ecotype or sub-ecotype taxonomic patterns occurring at very rapid time scales [33–37]. In the SCB, cold-water ecotypes *Synechococcus* Clade I and Clade IV have been shown to dominate most of the year, with intermittent incursions of the warm-water ecotype Clade II [33, 37, 38]. Thus, we predict that (i) cyanobacteria will be sensitive to climatically-forced environmental changes and (ii) shifts in diversity at specific phylogenetic levels and their associated traits will reveal how bacterioplankton experience these environmental changes.

Here, we use cyanobacterial populations to test whether microbial populations across differing levels of phylogenomic similarity show significant community changes in response to a prolonged warming period. To characterize microbial populations, we sequenced the highly variable cyanobacterial *rpoC1* gene [39] from weekly-to-monthly samples between 2009 and 2018 at the Newport Pier MICRO time series. We specifically predicted that (i) the abundance of *Prochlorococcus* relative to *Synechococcus* would increase in response to the El Niño

conditions, (ii) warming would result in an increase in the relative abundance of the high-temperature ecotypes of *Prochlorococcus* and *Synechococcus*, and (iii) changes in nutrient availability would result in systematic shifts in the composition of microdiverse populations over seasonal and annual time scales. This work has important implications for understanding how the link between phylogenetic trait distributions and microbial populations both dictates response to and reveals the impact of future anthropogenic ocean warming.

Materials and methods

Sample collection

Between September 2009 and 2018, 434 surface seawater samples were taken at varying temporal resolutions (i.e., daily to monthly) from the MICRO time series at Newport Pier in Newport Beach, California, USA (33.608°N and 117.928°W). In this observational field study no permits were required to collect seawater samples. Sample collection and processing were performed as previous [5, 23]. Briefly, two autoclaved bottles were rinsed with ocean water before collection and immediate transport. Replicate DNA samples were collected via filtration of 1 L of seawater through a 2.7 µm GF/D and a 0.22 µm polyethersulfone Sterivex filter (Millipore, Darmstadt, Germany) using sterilized tubing and a Masterflex peristaltic pump (Cole-Parmer, Vernon Hills, IL). DNA was preserved with 1620 µl of lysis buffer (23.4 mg/ml NaCl, 257 mg/ml sucrose, 50 mM Tris-HCl, 20 mM EDTA) and stored at -20°C. Nitrate and phosphate samples were collected in prewashed 50 mL Falcon tubes and filtered through a 0.2 µm syringe filter and stored at -20°C. Nutrient samples were analyzed at the Marine Science Institute at the University of California, Santa Barbara or at University of California, Irvine for measurement of NO₃⁻ and PO₄³⁻ as soluble reactive phosphorus (SRP). Finally, temperature was recorded via an automated shore station. The data was downloaded from the SCCOOS website for the data range 2009–2018. Environmental trends can be accessed via the MICRO BCO-DMO deployment (DOI:10.26008/1912/bco-dmo.564351.2).

DNA extraction and amplification

Bacterial DNA was extracted from Sterivex syringe filters (Millipore). The filters were incubated at 37°C for 30 minutes with lysozyme (50 mg/ml final concentration) before Proteinase K (1 mg/ml) and 10% SDS buffer were added and incubated at 55°C overnight. The DNA was precipitated using a solution of ice-cold isopropanol (100%) and sodium acetate (245 mg/ml, pH 5.2), pelleted via centrifuge, and resuspended in TE buffer (10 mM Tris-HCl, 1 mM EDTA) in a 37°C water bath for 30 min. DNA was purified using a genomic DNA Clean and Concentrator kit (Zymo Research Corp., Irvine, CA), and the concentration was quantified using a Qubit dsDNA HS Assay kit and Qubit fluorometer (ThermoFisher, Waltham, MA).

Sequencing of *rpoC1* Gene

Polymerase chain reaction (PCR) was used to amplify the cyanobacterial *rpoC1* gene using degenerative *rpoC1* primers, SAC1039R (5' - CYT GYT TNC CYT CDA TDA TRT) and 5M_newF (5' -GAR CAR ATH GTY TAY TTY A). A total of 4 ng DNA was added to 20 µl reactions [0.3 µM primers, 2.5 units 5-Prime HotMaster DNA Taq Polymerase (Quantabio, Beverly, MA), MasterAmp 1× Premix F (Epicenter Biotechnologies, Wisconsin, USA)].

Amplified samples from 2009–2013 were sequenced on a 454 Titanium platform (Roche, Switzerland). Amplification was performed with the following PCR steps: 95°C for 2 min, 10 cycles of 95°C for 30 s, 50°C for 40 s, and 72°C for 60 s. The resulting PCR product was retrieved and a forward primer with the Roche 454 Titanium flow cell adapter sequences and a

12 base pair Golay barcode sequence was added to the reaction at a concentration of 1 ng/ μ l. The barcoded sequences were amplified under the following conditions: 23 cycles of 95°C for 30 s, 50°C for 40 s, 72°C for 60 s, and a final extension step 72°C for 10 min.

Samples from 2014–2018 as well as select samples from 2011–2013 were sequenced using a MiSeq platform (Illumina, San Diego, CA) with 300 bp paired-end chemistry. Amplification occurred under the following conditions: 94°C for 2 min, 34 cycles of 94°C for 30 s, 48°C for 40 s, and 72°C for 60 s. Next, 1 μ l each of I5 and I7 Nextera v2 barcoded indices with Illumina adapters (1 ng/ μ l) were added to the PCR products. Annealing of the barcoded indices to the amplicon occurred as follows: 10 cycles of 94°C for 30 s, 55°C for 40 s, and 72°C for 60 s, and a final extension at 72°C for 10 min.

The resulting PCR product length was analyzed via agarose gel electrophoresis and the bar-coded products were pooled. Dimers that were less than 500 nucleotides long were then removed using magnetic bead purification (Agencourt AMPure XP beads, Beckman Coulter Inc., Brea, CA). Product purity and length distribution was checked using a 2100 Bioanalyzer high sensitivity DNA trace (Agilent, Santa Clara, CA). Roche 454 sequencing was performed using a 454 GS FLX+ Titanium (Roche, Basel, Switzerland) resulting in 323,143 reads. Illumina sequencing was performed using a MiSeq 300 bp paired-end platform with 600 cycles (Illumina, San Diego, CA) resulting in 14,492,986 reads. Sequence files are available from the NCBI Sequence Read Archive (accession #PRJNA624320).

Sequence analysis

Both 454 and Illumina sequences were quality filtered using the same processing steps. First, PhiX control sequences were removed using Bowtie 1.1.2. FASTQC was then used to determine where read quality dropped below Q20. The 454 reads were truncated to 385 bp and the Illumina forward reads were truncated to 255 bp. Next, fastq-mcf [40] was used to filter reads with a mean quality score below 20 or with more than 1% of bases below Q20. Finally, sequences were trimmed to the same 248 bp fragment (BioPython, v. 1.7.0, [41]). Quality filtered and truncated sequences were imported into QIIME 2 (v. 2.2018.11, [42]).

The 454 and Illumina demultiplexed sequences were denoised independently using the QIIME 2 command `dada2 denoise-single` with the following parameters (`—p-trunc-len 0—p-max-ee 3—p-n-reads-learn 800000`). Next, the datasets were merged and sequences were taxonomically identified using the `vsearch` classifier (default parameters) to compare sequences to a hand-curated database of 115 *Prochlorococcus*, *Synechococcus*, and other common marine bacterial reference genomes. Statistical analyses of taxonomic patterns were performed in the R computing environment [43]. Prior to calculations of ecotype relative abundance, samples were rarefied to a consistent sequencing depth of 3000 sequences per sample (“`rrarefy`” in the “`vegan`” package, [44]). A depth of 3000 was selected via the protocol outlined in [45]. Briefly, the species matrix was rarefied to a range of depths 10 times each, then both richness and Shannon’s diversity trends were compared to the overall dataset via Pearson correlation. A rarefaction depth of 3000 resulted in diversity trends that were > 95% similar to the overall dataset (S1 Fig). All samples were rarefied 100 times and the median count for each taxon in each sample was used in all relative abundance and temporal trend analyses.

To identify microdiverse populations, sequence feature IDs associated with known *Prochlorococcus* and *Synechococcus* reference genomes were used to extract and align ecotype-specific *rpoC1* sequences. Sequence codons were aligned (MEGA, version 7.0.21) and sequences with frameshift mutations were removed. The ecotype-specific majority sequence for each sample was calculated (BioPython) based on the 30% nucleotide consensus at each base pair position using all sequences associated with the ecotype of interest. Highly conserved single

nucleotide polymorphisms (SNPs) in the station-specific majority sequences were identified via comparison to the *rpoC1* sequence from a reference genome.

SNP-delineated microdiverse “haplotypes” were identified in one *Prochlorococcus* and one *Synechococcus* ecotype (HLI and Clade II). Specifically, aligned reads were used to calculate the pairwise Euclidean distance between all sequences (i.e., no. of nucleotide differences). This distance matrix was then clustered via average-linkage hierarchical clustering (“hclust” in the “stats” package). Within-cluster sum of squares was used to determine the optimum number of SNP clusters, then the stability of the SNP clusters was assessed via Jaccard bootstrapping (“cluster.stats” and “clusterboot” in the “fpc” package, [46]). Three basepair positions in the consensus sequence were used to distinguish between the two largest stable haplotype clusters for each ecotype (HLI: base pairs 9, 57, 108; Clade II: base pairs 48, 78, 81). Sequences from each sample that matched the haplotype-specific SNP profiles were counted and transformed into relative abundance by dividing by the sequence count for each ecotype.

Environmental trends

To quantify both seasonal and interannual trends in the environment and microbial community, we fit the following ANOVA model to our data:

$$Y_{ijk} = \mu + \alpha_{Year}X_{Year,j} + \beta_{Month}X_{Month,k} + \varepsilon_{ijk} \quad (1)$$

Specifically, we performed Type II ANOVAs on categorical linear regressions of temperature, nitrate, phosphate, or relative clade abundance observations (Y_{ijk}) as a function of year (X_j) and month (X_k) with corresponding regression coefficients (i.e., treatment effects) α_{Year} and β_{Month} . Thus, in this manuscript α_N represents the annual nitrate trend, and β_P represents the monthly phosphate trend, etc. We used the “Anova” function in the “car” package [47] and the “lm” function in the “stats” package of R to perform this analysis.

Results

We tested the prediction that warming and declining nutrient supply in the Southern California Bight (SCB) would result in an increase in the oligotrophic ecotypes of *Prochlorococcus* and *Synechococcus*. Therefore, we collected temperature, nutrient, and microbial genomic DNA samples for *rpoC1* gene sequencing at 434 time points from 9 September 2009 to 5 December 2018 as a part of the Newport Beach Pier MICRO time series (33.608°N, 117.928°W). Specifically, we compared the effects of seasonal and interannual environmental variability on microbial populations at the genus, ecotype, and microdiverse phylogenomic level.

Decomposing environmental variability

As reported in Martiny *et al.* 2016 and Fagan *et al.* 2019, temperature and inorganic nutrient concentrations showed significant seasonal and interannual variability across the MICRO time series. To lend context to our novel cyanobacterial population trends, here we add environmental information for 2018 (Fig 1A). Both month and year of sampling had a significant effect on the observed environmental patterns, demonstrating both seasonality and interannual variation (Table 1). Temperature and nutrient concentrations were anti-correlated across the seasonal cycle. Nutrient concentrations were highest in the Winter and Spring, whereas temperature was highest in the Summer and Fall (Fig 1A and 1C). However, these trends became partially decoupled across multi-year scales. Specifically, temperature and nitrate both showed decreasing trends in 2013 (Fig 1C). Next, nitrate continued to decrease but temperature rose sharply in 2014–2015. Temperature began to decrease in 2016 concurrently with an

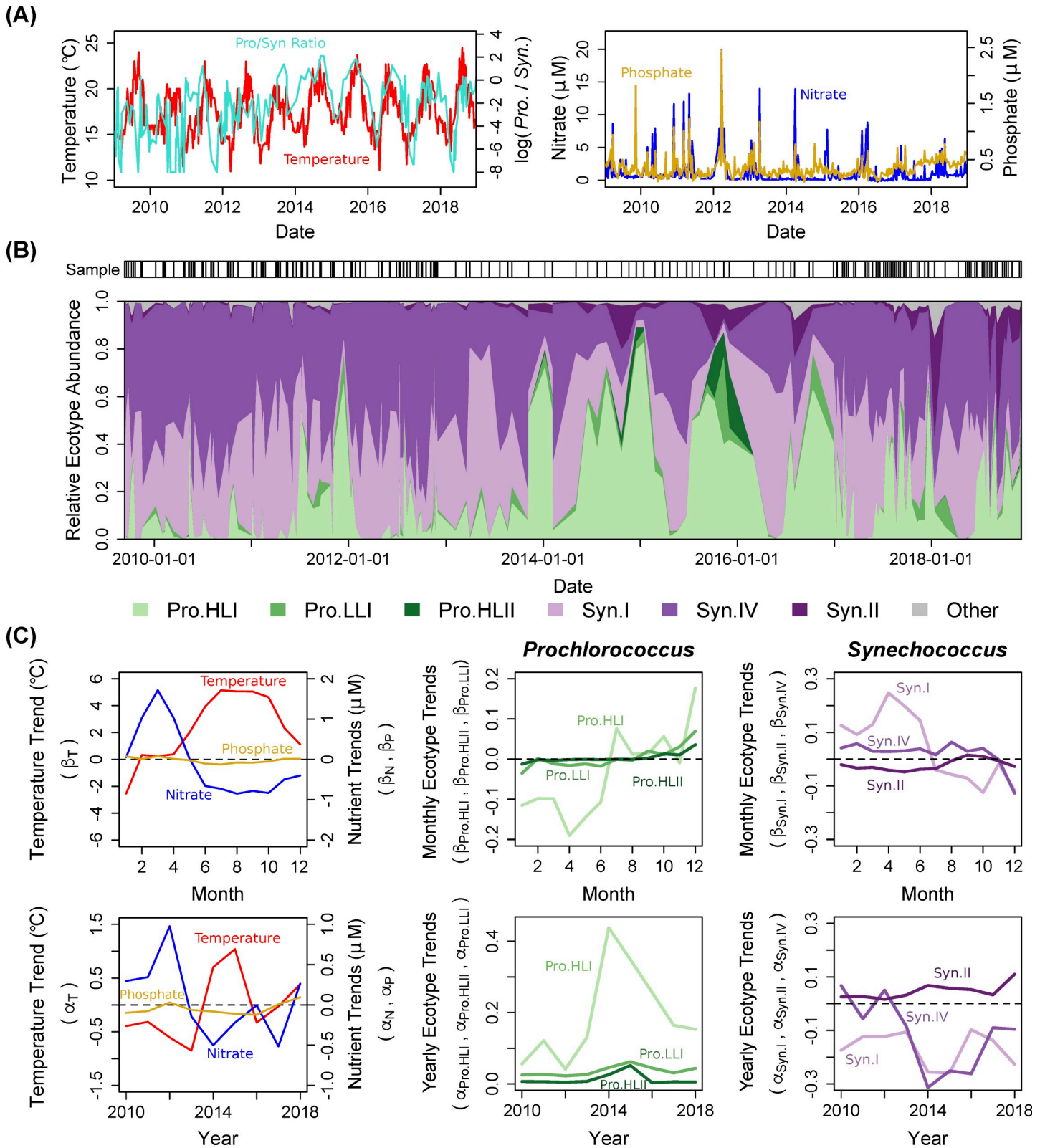


Fig 1. Seasonal and interannual changes in environmental conditions and ecotype frequencies. (A) Temperature (°C), nitrate and phosphate concentrations (μM), and the log₁₀-transformed ratio of *Prochlorococcus* sequence counts relative to *Synechococcus* sequence counts in the MICRO time series. (B) Interpolated relative abundance of *rpoC1* reads taxonomically assigned to the six most abundant *Prochlorococcus* (Pro.) and *Synechococcus* (Syn.) ecotypes. The sampling dates are marked

along the top of the time series. (C) Linear model regression coefficients for environmental variables and relative ecotype abundance as a function month and year (see [Methods](#)). A trend of 0 is marked with horizontal dashed lines.

<https://doi.org/10.1371/journal.pone.0238405.g001>

increase in nitrate, but these trends reversed in 2017. Here, we additionally report that both temperature and nitrate had increasing trends in 2018. In contrast, phosphate had a decreasing trend throughout most of the time series with slight increases in 2012, 2017, and 2018. As a result, the warmest years were 2014, 2015 and 2018, but whereas low nutrient concentrations were observed in 2014–2015, 2018 had relatively high inorganic nutrients. Overall, these results support the conclusion that El Niño peaked in 2015 [5, 23, 48]. However, nitrate began to decrease at the sampling site prior to the marine heatwave, suggesting that multiple physical oceanographic or anthropogenic processes could have regulated the environmental changes at this location.

Shifts in cyanobacteria lineages

The ratio of *Prochlorococcus* to *Synechococcus* reads also showed significant seasonal and inter-annual trends. In an ANOVA model, month and year explained a combined 47% of the variance in the *Prochlorococcus/Synechococcus* ratio (Table 1). On a seasonal cycle, this ratio had its highest increase in the early Winter concurrent with decreasing temperature (S2 Fig). However, the ratio increased across all 9 years of the transect (S2 Fig). The largest increases in the *Prochlorococcus/Synechococcus* ratio were observed in 2014 and 2015 with the onset of low inorganic nutrient conditions and El Niño. A similar shift from a *Synechococcus*-dominated system to an increased abundance of *Prochlorococcus* was also observed using flow cytometry [5]. As seen in other studies [3], there was a significant relationship between the sequence read ratio and the cell count ratio when DNA and flow cytometry samples were collected simultaneously (S3 Fig). This ratio was not dependent on sequencing platform but both platforms overestimated the ratio of *Prochlorococcus* to *Synechococcus* reads when *Prochlorococcus* cell counts were below 15 cells/ml (S3 Fig). Thus, the sequence and cell counts were mostly correlated and suggested an increase in the *Prochlorococcus/Synechococcus* ratio and an increasingly oligotrophic system.

Table 1. Type II ANOVA results relating seasonality and interannual variability to environmental trends.

	Total	Month	Year	Month	Year	Adjusted
	SS	SS	SS	P-Value	P-Value	R ²
Temperature	3255.39	2091.83	160.35	< 0.001	< 0.001	0.68
Nitrate	2157.63	331.79	80.48	< 0.001	0.015	0.16
Phosphate	17.69	1.67	2.07	< 0.001	< 0.001	0.18
Pro/Syn Ratio	1200.51	366.46	259.23	< 0.001	< 0.001	0.47
Pro.HLI	7.63	1.55	2.10	< 0.001	< 0.001	0.44
Pro.HLII	0.35	0.07	0.03	0.004	< 0.001	0.28
Pro.LLI	0.12	0.01	0.03	< 0.001	0.015	0.21
Syn.I	7.03	2.53	0.64	< 0.001	0.001	0.39
Syn.IV	6.12	0.24	2.25	0.38	< 0.001	0.37
Syn.II	0.69	0.08	0.17	0.001	< 0.001	0.29
Pro.HLI.2	44.01	1.10	21.85	0.15	< 0.001	0.51
Syn.II.2	28.49	2.53	10.93	0.03	< 0.001	0.44

Seasonality (month) and interannual variability (year) each have a significant effect on almost every variable examined, including environmental patterns, the ratio of *Prochlorococcus/Synechococcus*, and the relative abundance of cyanobacterial taxa. SS = Sum of Squares.

<https://doi.org/10.1371/journal.pone.0238405.t001>

Ecotype level trends

During the 2014–2016 SCB marine heatwave, we observed an increase in the relative abundance of *Prochlorococcus* and *Synechococcus* ecotypes commonly associated with high temperature conditions. Month and year explained between 21–44% of the variance in relative ecotype abundance across the MICRO time series (Table 1). On seasonal time scales, *Synechococcus* Clade I increased in the Spring (~Feb.-Jun.), *Synechococcus* Clade II and *Prochlorococcus* High Light I (HLI) increased in the Summer and Fall (~Jul.-Oct.), and *Prochlorococcus* Low Light I (LLI) and High Light II (HLII) demonstrated slight increases in the Winter (Dec.) (Fig 1C). Only the *Synechococcus* Clade IV ecotype did not show significant monthly variability (Table 1).

At annual time-scales, the system was initially dominated by the cold-water *Synechococcus* ecotypes Clade I and Clade IV [28] (Fig 1B). However, in 2014, there was a large increase in the relative abundance of *Prochlorococcus* cooler water ecotype HLI [27] as well as a slight increase in the relative abundance of the warm-water *Synechococcus* Clade II. Moreover, at the peak of El Niño in the fall of 2015, we detected the high-light, high-temperature *Prochlorococcus* ecotype HLII. As the marine heatwave abated in 2017, *Synechococcus* Clade II persisted in the system but *Prochlorococcus* HLII disappeared. Overall, Clade II and all *Prochlorococcus* ecotypes had an increasing trend throughout the entire time series, with the highest frequencies seen during the 2014–2015 El Niño period (Fig 1C). Conversely, Clade I and Clade IV largely had decreasing trends across the time series. In sum, relative ecotype abundance showed systematic seasonal and interannual variability that partially aligned with environmental trends in temperature and nutrients.

Relative ecotype abundance trends generally showed significant correspondence with changes in temperature and inorganic nutrients. However, the strength of each relationship was dependent on the temporal factor and the taxa level examined (Fig 2; for data associated with Fig 2 see S1 Table). We wanted to determine whether the non-independent relationship between the relative abundance of *Prochlorococcus* and *Synechococcus* influenced their apparent temporal trends. Therefore, we examined the relative abundance of the ecotypes normalized to all Cyanobacteria ($Pro_{All} = Pro_{Ecotype\ Abundance} / (Pro_{Abundance} + Syn_{Abundance})$ and $Syn_{All} = Syn_{Ecotype\ Abundance} / (Pro_{Abundance} + Syn_{Abundance})$) versus normalized to within *Prochlorococcus* ($Pro_{Within} = Pro_{Ecotype\ Abundance} / Pro_{Abundance}$) or *Synechococcus* ($Syn_{Within} = Syn_{Ecotype\ Abundance} / Syn_{Abundance}$). In almost all cases, the link between ecotype trend and environmental trend was the same for both Syn_{All} and Syn_{Within} (Fig 2). In contrast, Pro_{All} and Pro_{Within} showed very different correlations depending on the normalization. HLI, LLI, and HLII all increased relative to the major *Synechococcus* clades (i.e., I and IV). However, the trend was more complicated within *Prochlorococcus*, where LLI and HLII showed non-linear relationships with HLI. Thus, the observed trends were dependent on the phylogenomic level of the analysis. On a seasonal cycle, when examining the within-genus trends, HLI and Clade IV had significant positive correlations with temperature trends; LLI had a significant positive correlation with phosphate trends; Clade I had a significant positive correlation with nitrate trends; and Clade IV had a significant negative correlation with nitrate trends (Fig 2). Across all Cyanobacteria on an interannual scale, Clade I had a significant negative relationship and all *Prochlorococcus* ecotypes had significant positive relationships with temperature trends. Within *Synechococcus*, Clade II had a significant positive correlation with interannual temperature trends. Additionally, HLI had a significant negative and Clade IV had a significant positive correlation with nitrate interannually. There were no significant correlations between interannual phosphate and ecotype trends. Overall, temperature trends had a stronger relationship with relative ecotype abundance across years, whereas nitrate had a similar

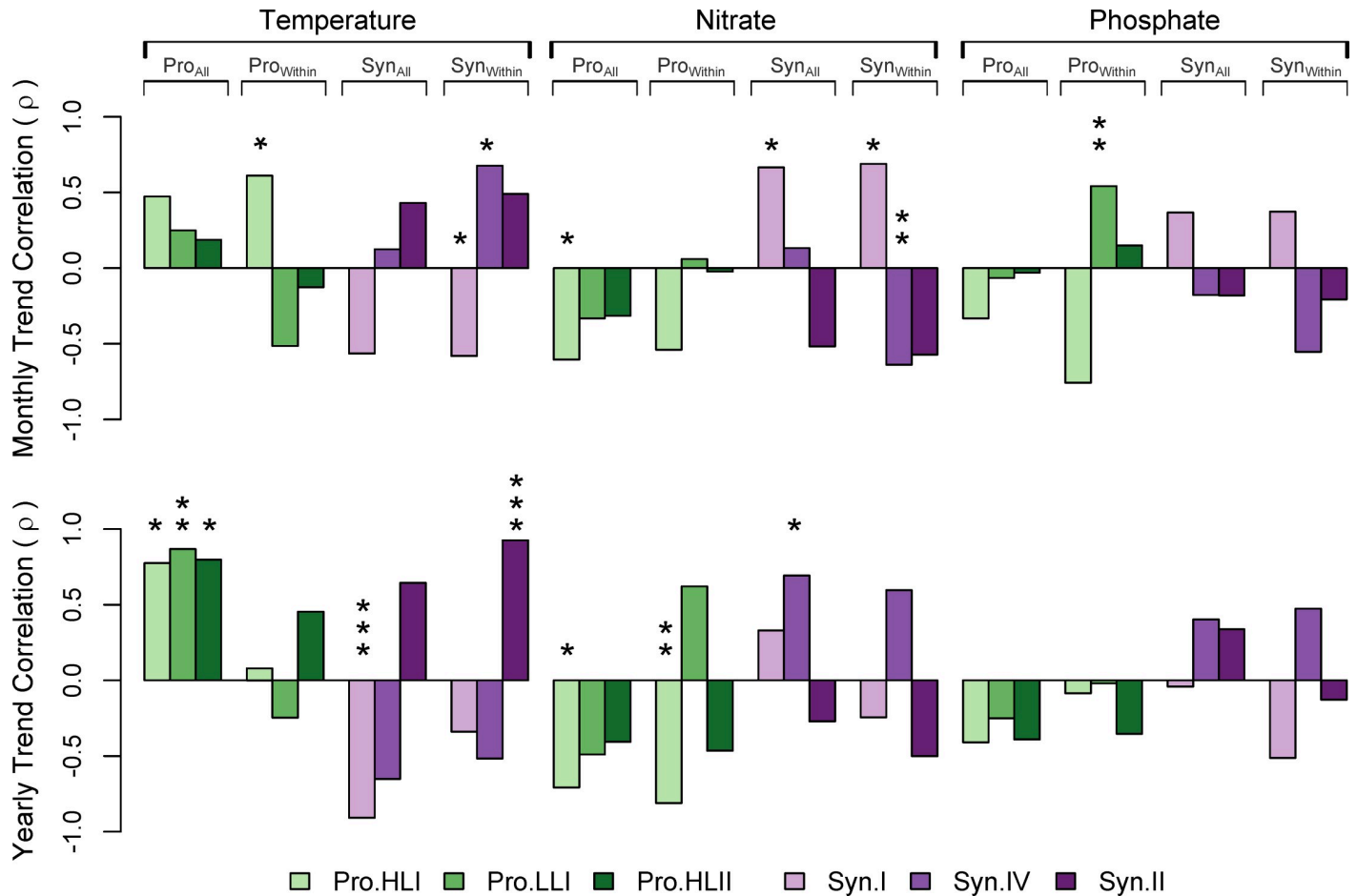


Fig 2. Pearson correlation coefficients (r) between relative abundance trends and environmental trends. The significance of each correlation is marked as p -value: * < 0.05, ** < 0.01, *** < 0.001. Bars without a mark had a non-significant correlation.

<https://doi.org/10.1371/journal.pone.0238405.g002>

relationship with the ecotype trends across months and years, suggesting that the effects of changing nitrate and temperature operate on different temporal scales.

Microdiversity trends

Most microdiverse *Synechococcus* and *Prochlorococcus* populations were dominated by a single SNP-delineated population across the time series. We identified microdiverse populations (i.e. “haplotypes”) based on conserved single nucleotide polymorphisms (SNPs) in the *rpoC1* gene (Fig 3). A limited set of closely related haplotypes were present in four of the six most abundant ecotypes (LLI, HLII, Clade I and Clade IV) across all seasons and years. Stable SNPs were particularly prominent for the *Synechococcus* Clade I (Fig 3). Conversely, the *Synechococcus* Clade IV and *Prochlorococcus* LLI ecotypes had few unique SNPs across the time series. The final ecotype with a single dominant haplotype, *Prochlorococcus* HLII, had a highly stochastic distribution of SNPs, which may be influenced by its generally low sequence counts and associated sequencing errors. In contrast, there were clear shifts in *Prochlorococcus* HLI and *Synechococcus* II haplotypes.

The SCB marine heatwave appeared to induce shifts in the relative abundance of *Prochlorococcus* HLI and *Synechococcus* II haplotypes. For both HLI and Clade II, two statistically stable

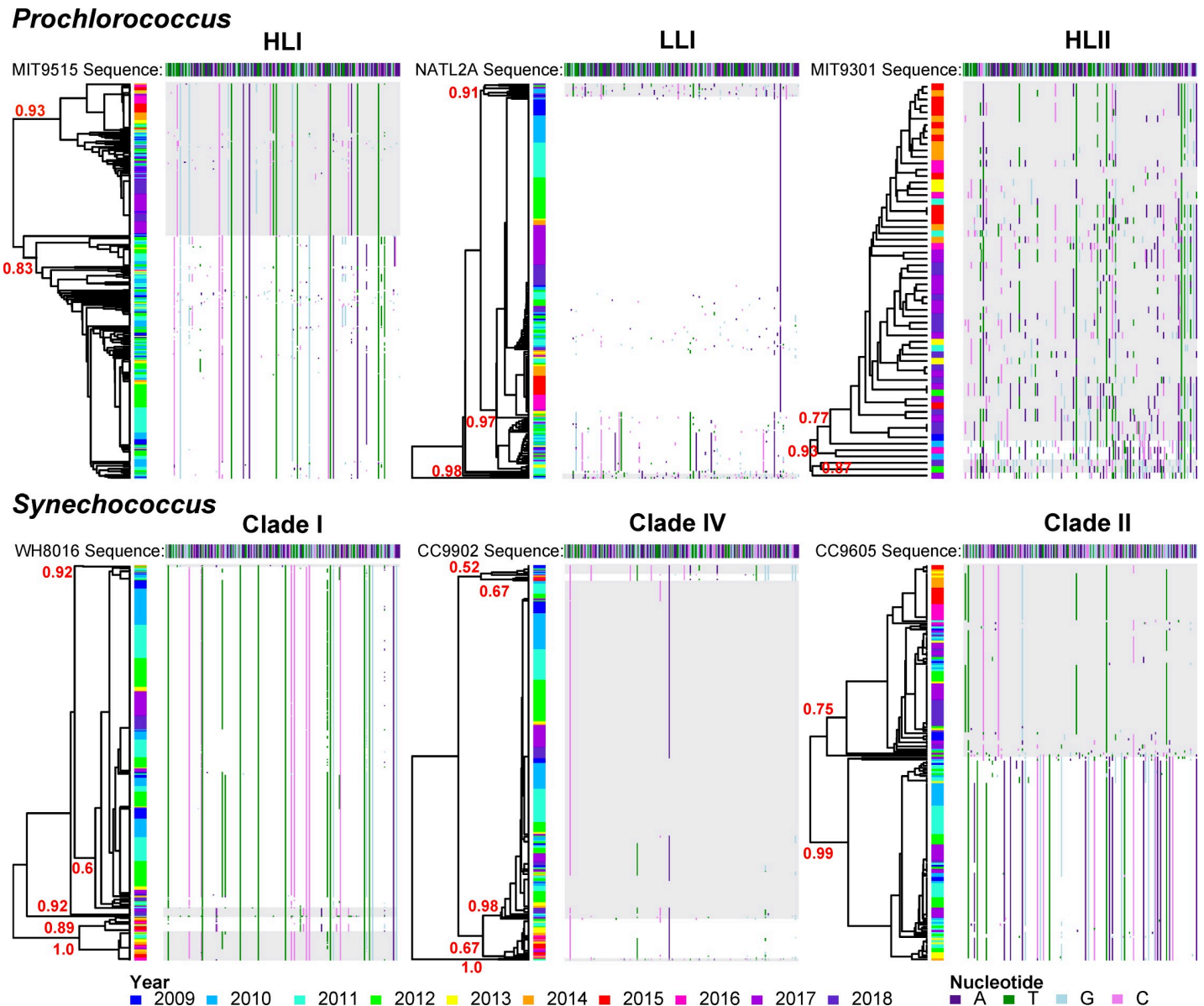


Fig 3. Microdiversity clusters within the most abundant *Prochlorococcus* and *Synechococcus* ecotypes were temporally and statistically stable. Dendrograms represent the average-linkage hierarchical clustering of single nucleotide polymorphisms (SNP) differences between a *rpoC1* reference sequence and the majority consensus sequence at each sampling time point. Each row of the dendrogram represents the consensus *rpoC1* sequence at a time point, where only SNPs (in comparison to the reference sequence) are depicted. Only time points where the ecotype was present are shown. The reference *rpoC1* sequence is depicted at the top of each dendrogram. Reference genomes used to compare *rpoC1* sequences included: HLI-MIT9515; LLI-NATL2A; HLII-MIT9301; Clade I-WH8016; Clade IV-CC9902; and, Clade II-CC9605. Within-cluster sum of squares was used to determine the optimum number of SNP-based clusters (i.e., haplotypes). Cluster labels (red) indicate bootstrapped Jaccard similarity values for the most stable clusters (values < 0.5 are unstable, 0.6–0.75 weak stability, 0.75–0.85 stable, and > 0.85 highly stable). Stable clusters are alternately shaded in grey for emphasis.

<https://doi.org/10.1371/journal.pone.0238405.g003>

haplotypes were identified (Fig 4). On average 90.2% of the HLI and 99.8% Clade II reads were associated with one of two haplotypes, respectively. The two *Synechococcus* Clade II haplotypes, but not the *Prochlorococcus* HLI haplotypes, showed significant seasonal variability (Table 1 and Fig 4B). The haplotypes Pro.HLI.1 and Syn.II.1 were frequent from the Spring/Summer of 2010 through the Summer/Fall of 2012 (Fig 4A). During this time, the second haplotypes (Pro.HLI.2 and Syn.II.2) appeared during short periods. However, starting in 2013–

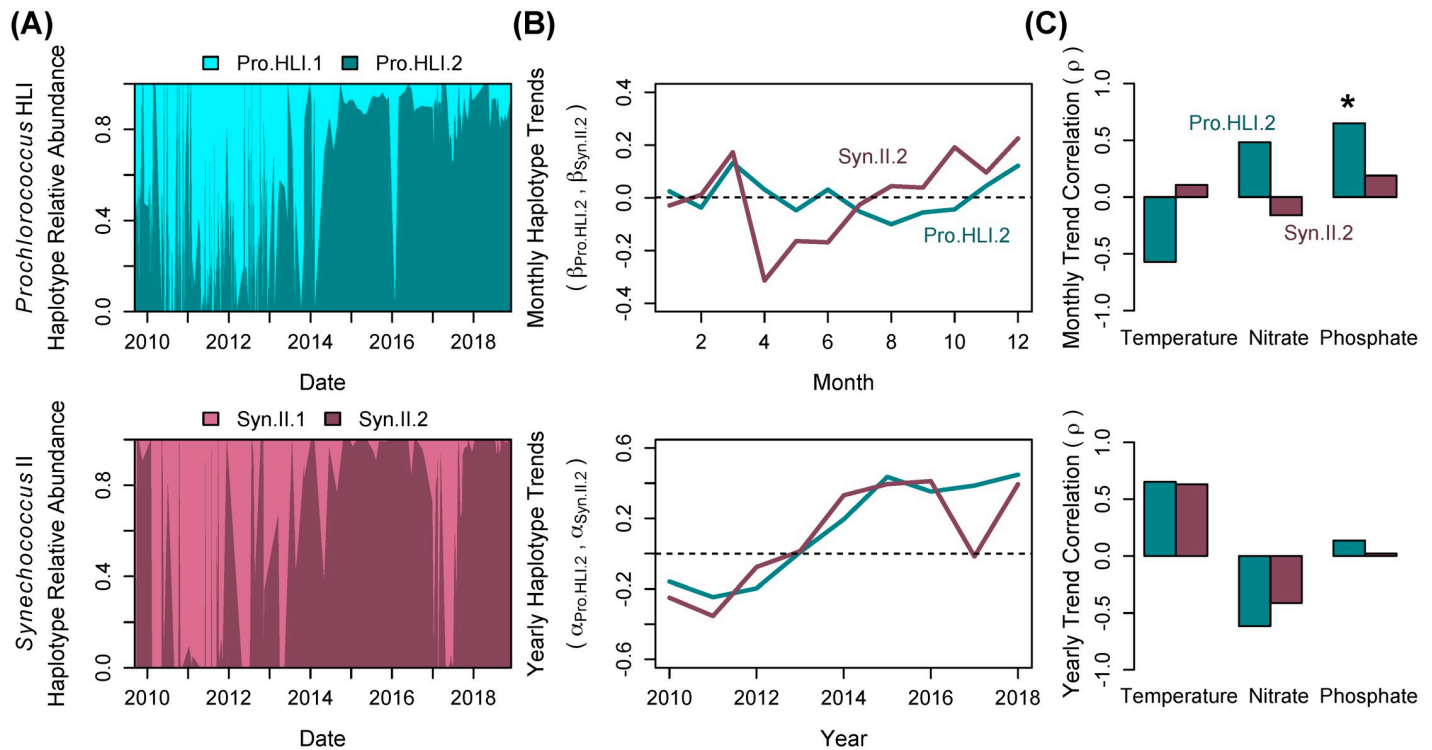


Fig 4. *Prochlorococcus* HLI haplotypes (Pro.HLI.1 and Pro.HLI.2) and *Synechococcus* II haplotypes (Syn.II.1 and Syn.II.2) showed significant shifts in composition across the time series. (A) Interpolated relative abundance of the haplotypes. Samples with less than 10 reads were removed from the analysis. (B) Linear regression coefficients for monthly and yearly trends in the Pro.HLI.2 and Syn.II.2 haplotypes. (C) Pearson's correlation coefficients (ρ) comparing haplotype to environmental monthly and yearly trends. The significance of each correlation is marked as p -value: * < 0.05 . Bars without a mark had a non-significant correlation.

<https://doi.org/10.1371/journal.pone.0238405.g004>

2014, Pro.HLI.2 and Syn.II.2 rose in frequency (Fig 4B). A systematic reversal of this trend occurred briefly for *Synechococcus* II in the first half of 2017, when Syn.II.2 decreased in relative abundance before increasing again in 2018. The Pro.HLI.2 and Syn.II.2 seasonal and inter-annual patterns were also compared to the trends in environmental parameters, but only phosphate had a significant correlation with seasonal HLI haplotype trends (Fig 4C). Comparisons to trends in the ratio of inorganic nitrate:phosphate were also non-significant (data not shown). Thus, although year of sampling had a strong influence on relative haplotype abundance, interannual changes in the dominant haplotype could not be attributed to a specific environmental factor.

Testing for endemism among warm water ecotypes

The contrast between ecotypes with stable versus variable haplotypes raised the question as to whether some haplotypes were endemic to our study site. Alternatively, they may have represented populations physically transported from the broader eastern Pacific Ocean. To place the microdiversity of our warm water ecotypes in the context of other Pacific Ocean regions, we compared our *Prochlorococcus* HLII and *Synechococcus* Clade II haplotypes to previously collected surface samples from the central Pacific Ocean [49]. For HLII, the majority of samples taken from gyre and equatorial regions clustered separately from the MICRO samples (Fig 5). However, 12 of the Newport samples were a part of stable clusters that included the open ocean samples. Although these samples showed similar SNPs, they did not have similar *in situ* temperature or nitrate concentrations. For Clade II, equatorial samples with high nitrate

concentrations clustered separately but were most closely related to the Syn.II.1 haplotype. In contrast, Clade II samples from the low nutrient, high temperature North Pacific Subtropical Gyre clustered with the Syn.II.2 haplotype, which was most abundant later in the time series. This result suggests that the microdiversity of populations observed in the SCB is at least partially connected to other locations in the Pacific Ocean.

Discussion

Our data suggests that long-term warming in the Southern California Bight initiated a significant change in picocyanobacteria populations that persisted for 2–5 years (Fig 1). In contrast, zooplankton communities typically return to pre-El Niño states within 1–2 years [24]. Although “alternative stable states” have been documented in macroecology [50, 51], few studies have reported persistent changes in microbial communities [52, 53]. Stable, long-term shifts in microbial composition have generally been driven by changes in conditions linked to deeply conserved traits such as shifts from iron-reduction to sulfate-reduction [54], oxic to anoxic conditions [55], or increased photoinhibition [56]. In the marine environment, multi-centennial changes in temperature and nutrient availability may have led to shifts in the abundance of N₂-fixing cyanobacteria in the North Pacific Subtropical Gyre (NPSG) [9]. Moreover, a polarity reversal of the Pacific Decadal Oscillation in 1976 may have caused increased mixed layer stratification and shoaling, decreased nutrient availability, and a regime shift from a eukaryote- to a prokaryote-dominated system in the central Pacific Ocean [57]. In the MICRO time series, the marine heatwave of 2014–2016 and concurrent 2015 El Niño resulted in an increase in ecotypes associated with warmer conditions including *Prochlorococcus* HLI, LLI, and HLII as well as *Synechococcus* Clade II (Fig 1). Moreover, the HLI and Clade II microdiverse haplotypes demonstrated persistent, altered community composition in response to the 2015 El Niño disturbance (Fig 4A). Here, similar processes as those observed in the NPSG may be operating concurrently to drive community composition changes in the SCB.

Given the systematic and persistent changes in Cyanobacteria populations in the SCB, what are the ecosystem processes driving this shift in microbial communities? Both *Prochlorococcus* as a whole, which is more abundant in high temperature biomes than *Synechococcus* [58], and the *Synechococcus* high temperature Clade II increased in relative abundance across the entire time series (Fig 1 and S2 Fig). In addition, it is well-documented that 20°C represents a temperature threshold above which *Prochlorococcus* HLII outpaces HLI ecotype growth [27, 59]. At MICRO, *in situ* temperatures were above 20°C for greater than 20.8% of dates in 2014, 2015, 2017, and 2018 and less than 14.2% of dates in 2010–2013 and 2016. Thus, the increased abundance of all *Prochlorococcus*, *Prochlorococcus* HLII, and *Synechococcus* Clade II may all reflect this warming. However, the *Prochlorococcus*/*Synechococcus* ratio as well as HLII relative abundance peaked in the winter (Fig 1 and S2 Fig). Additionally, the within-genus HLII monthly trends were negatively correlated with temperature (Fig 2). These results may indicate an important role of regional warming and advection of both oligotrophic water and microbial communities into the SCB [5, 23]. The 2015 El Niño event was one of the strongest on record in terms of broad-scale regional warming, even though reductions in upwelling and upwelling-favorable winds were relatively weak in comparison to previous, strong El Niño events such as 1982–1983 and 1997–1998 [48]. In addition, the SCB represents a transition zone between the southward California Current (CC) and the northward California Undercurrent (CUC). Thus, relatively small changes in source waters for the SCB may significantly change microbial populations. An increase in the northward CUC signal in SCB waters was observed between 1984–2012 [25]. The CC is characterized by cold, low-salinity, nutrient-poor “young” temperate water, whereas the CUC has high-salinity, nutrient-rich “old” equatorial waters

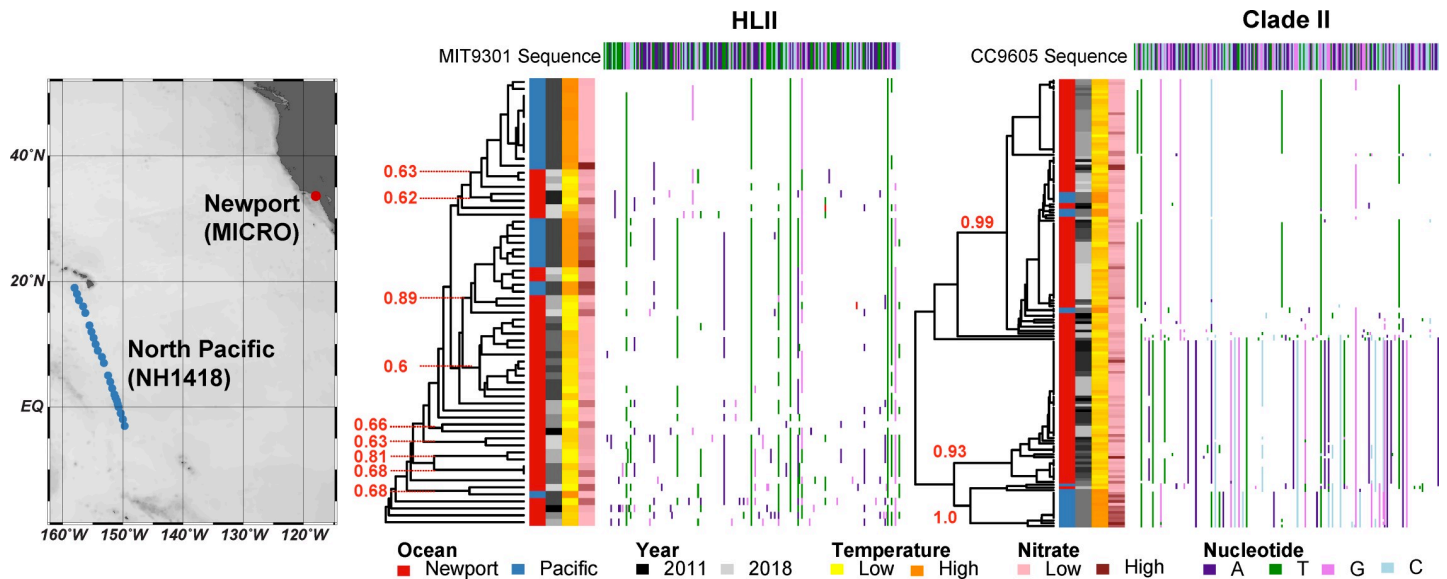


Fig 5. Comparison of *Prochlorococcus* HLII and *Synechococcus* Clade II *rpoC1* highly conserved SNPs detected at the Newport MICRO times series and on Pacific Ocean cruise NH1418 (September–October 2014; 19.00°N, -158.00°W to -3.00°N, -149.67°W; 5m depth). Newport and NH1418 samples largely clustered separately but had some overlap in SNPs. Samples with less than 10 sequences were removed from the analysis. Clade labels (red) indicate bootstrapped Jaccard similarity values for the most stable clusters with more than two samples (values < 0.5 are unstable, 0.6–0.75 weak stability, 0.75–0.85 stable, and > 0.85 highly stable).

<https://doi.org/10.1371/journal.pone.0238405.g005>

[60]. Therefore, changes in water mass may result in the influx of oligotrophic communities with a higher abundance of *Prochlorococcus* cells from the HLII ecotype. Comparison of microdiverse HLII and Clade II populations at MICRO and in the NPSG supports the conclusion that these populations are phylogenomically linked (Fig 5). We hypothesize that an increased percentage of high-temperature days locally but also a larger-scale regional warming trend that promotes the advection of oligotrophic populations into the SCB, contribute to a shifting picocyanobacteria community at MICRO.

There are several important caveats to our conclusions including the application of multiple sequencing platforms and temporal co-variance between environmental factors. The sequencing platform was partially associated with year of sampling and thus confounded with the shift in *Prochlorococcus/Synechococcus* sequence read ratios. However, the relationship between the sequence read ratio and the cell count-ratio of *Prochlorococcus/Synechococcus* was not dependent on sequencing platform (S3 Fig). Moreover, out of the six instances of samples collected with 48 hours but sequenced on different platforms, only one date showed significantly different ecotype frequencies between 454 and Illumina (S4 Fig). Previous studies have similarly shown that the ratio of major marine microbial taxa is consistent across genomic platforms [61]. In addition, a large number of highly conserved SNPs in the *rpoC1* consensus sequences were observed throughout the time series, regardless of sequencing platform (Fig 3). Rapid changes in sequencing platforms and technology, both in terms of read length and depth of coverage, are likely to continue into the future. Our analysis suggests that conserved SNPs can be integrated across platforms. The strong seasonal co-variance of multiple environmental factors also makes it challenging to separate the effects of temperature and nutrient concentrations on picocyanobacteria populations. However, our multi-year sampling regime partially addressed this issue as temperature and nutrient concentrations were less correlated at this time-scale. Overall, temperature disturbances including the El Niño event, the partial interannual decoupling of environmental trends, and the prevalence of stable microdiversity across

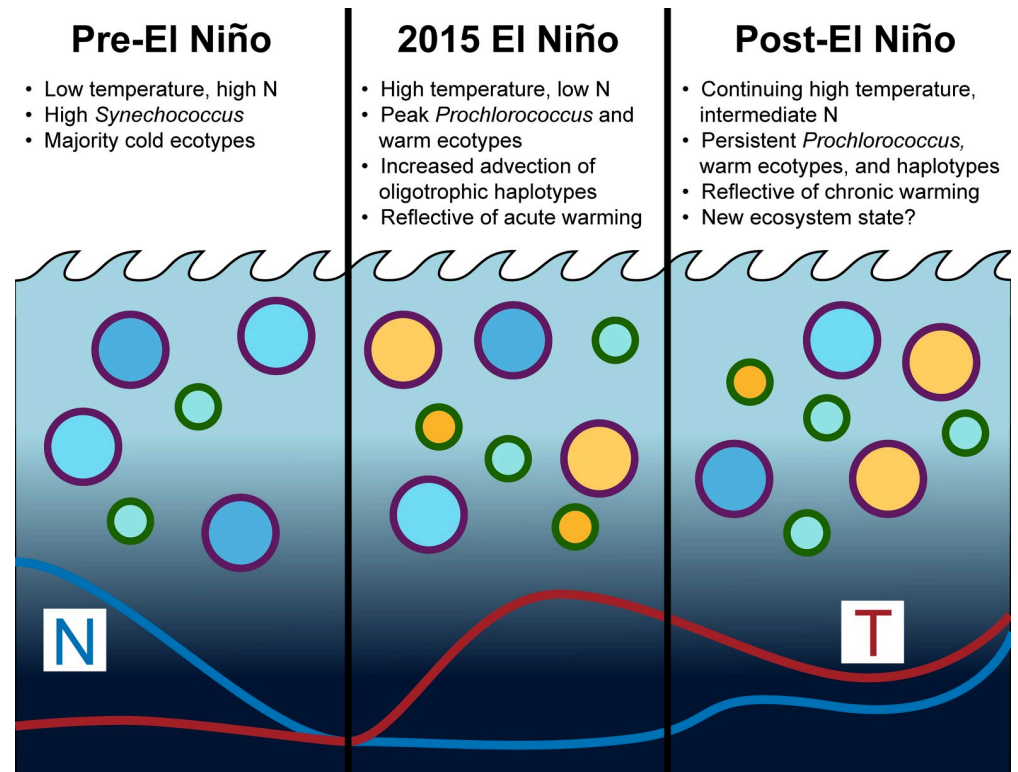


Fig 6. Conceptual diagram of picocyanobacterial community shifts at the MICRO time series from 2009–2018. *Synechococcus* cells are outlined in purple and *Prochlorococcus* cells are outlined in green. Blue cell shading indicates cold temperature-adapted ecotypes and yellow cell shading indicates warm temperature-adapted ecotypes. The blue line indicates the nitrate trend (N) and the red line indicates the temperature trend (T).

<https://doi.org/10.1371/journal.pone.0238405.g006>

the 9 years of the MICRO time series has made it an excellent natural laboratory to study the effects of climatic shifts on microbial populations.

The MICRO picocyanobacteria time series illustrates how we can “bi-directionally” link shifts in microbial diversity and environmental conditions to develop a deeper understanding of the impact of global changes. Past studies have revealed a rich understanding of the phylogenetic conservatism of response traits in microbial populations [62–64]. One of the main trait differences between the *Prochlorococcus* and *Synechococcus* genera is cell size, which results in a competitive advantage of *Prochlorococcus* under warm, low nutrient conditions [65]. Within the genera, it is also well-established that different light, temperature, and iron response traits are linked to specific ecotypes [27–29, 66]. In contrast, responses to biotic interactions, subtle temperature shifts, and nutrient supply ratios have been associated with microdiverse clades [30, 49, 67, 68]. *Prochlorococcus* and *Synechococcus* responses to environmental change at MICRO generally conformed to the phylogenomically predicted response at the genus and ecotype level (Fig 6). *Prochlorococcus* likely increased relative to *Synechococcus* across the time series due to traits conferring a competitive advantage in warm, oligotrophic conditions. Similarly, on annual scales, HLI, HLII, and Clade II likely increased over *Synechococcus* Clade I and Clade IV due to traits related to high temperatures and low nutrient concentrations [28]. However, several responses to environmental change did not conform to our knowledge of expected response traits. *Prochlorococcus* HLII and *Synechococcus* Clade IV showed a seasonally negative and positive correlation with temperature, respectively, and thus a divergent trend

compared to past studies. We attribute these unexpected observations to advection of genotypes from the broader eastern Pacific Ocean region that is also experienced warming. Overall, we saw limited changes at the microdiversity level, suggesting that the effect of shifts in environmental conditions or biotic interactions [37, 49, 69] were muted for most haplotypes here. However, some of these processes likely elicited the large responses in HLI and Clade II haplotypes observed in 2014–2015 (Fig 4), which supports our conclusion of a persistent shift in picocyanobacteria populations. It is too early to state whether this shift is indicative of a new ecosystem state in terms of nutrients, temperature, and cyanobacteria (Fig 6), but future time series efforts should continue to monitor climatic changes in the SCB. Global climate change is expected to have a complex impact on marine microorganisms as a result of nonlinear biophysical interactions between environmental conditions [70, 71]. Shifts in microbial populations and their traits can act as a “biosensor” and allow us to develop a stronger understanding of how climatic changes affect ecosystem functioning.

Supporting information

S1 Fig. Comparison of taxa richness (no. of taxa) and diversity (Shannon’s Diversity Index) in rarefied datasets to the overall dataset revealed high correlations (Pearson’s correlation coefficient of determination, r^2). Amplicon datasets were rarefied to a range of depths 10 times each and the correlation between each rarefaction and overall dataset was calculated. A rarefaction depth of 3000 sequences was selected for relative abundance analysis as it was the minimum depth at which all correlations had $r^2 > 0.95$.

(TIFF)

S2 Fig. Linear model regression coefficients for the \log_{10} -transformed ratio of *Prochlorococcus* sequence counts relative to *Synechococcus* sequence counts in the MICRO time series as a function month and year (see Methods). A trend of 0 is marked with horizontal dashed lines. The *Prochlorococcus*/*Synechococcus* ratio shows significant seasonal variability and has an increasing trend across all years of the study.

(TIFF)

S3 Fig. Comparison of the \log_{10} -transformed (*Prochlorococcus* + 1)/(*Synechococcus* + 1) ratio calculated by sequence read count and by flow cytometry cell count shows concordant patterns in the MICRO time series. (A) Sequence read ratio across the MICRO time series. Either a Roche 454 (purple) or an Illumina MiSeq (red) platform was used to sequence the *rpoC1* gene. (B) Cell count ratio from 2012–2015. Flow cytometry data was collected as in Martiny *et al.* (2016) [5]. (C) Comparison of read count ratios and cell count ratios in samples where DNA and flow cytometry were collected concurrently. When *Prochlorococcus* cellular abundance was above 15 cells/ml, the sequence ratio showed a significant linear relationship (blue line) with the cell count ratio (p -value < 0.001 , $R^2 = 0.48$).

(TIFF)

S4 Fig. Relative ecotype abundance for select MICRO samples collected within a two-day window and sequenced on a Roche 454 versus an Illumina MiSeq. The distribution of ecotype frequencies between sequencing platforms was compared using Pearson’s chi-square test for homogeneity (10000 permutations, * = p -value < 0.05). The distribution of ecotype frequencies was only significantly different between sequencing platforms for 1 out of 6 comparisons (R = Roche 454, I = Illumina MiSeq).

(PDF)

S1 Table. Pearson's correlation coefficients (r) and corresponding p -values for the comparison of seasonal (month) and interannual (year) environmental trends to taxa-specific trends.

(DOCX)

Acknowledgments

The authors would like to thank the large number of individuals who have contributed to collecting data for the MICRO time series including, but not limited to, Celine Mouginit, Stephen Hatosy, Jeremy Huang, Tanya Lam, Sarah Bowen, and the Allison Lab at the University of California Irvine.

Author Contributions

Conceptualization: Alyse A. Larkin, Adam C. Martiny.

Data curation: Alyse A. Larkin, Allison R. Moreno, Adam J. Fagan.

Formal analysis: Alyse A. Larkin.

Funding acquisition: Adam C. Martiny.

Investigation: Alyse A. Larkin, Allison R. Moreno, Adam J. Fagan, Alyssa Fowlds, Alani Ruiz.

Methodology: Alyse A. Larkin.

Project administration: Alyse A. Larkin, Adam C. Martiny.

Software: Alyse A. Larkin.

Supervision: Alyse A. Larkin, Allison R. Moreno, Adam C. Martiny.

Validation: Alyse A. Larkin, Adam C. Martiny.

Visualization: Alyse A. Larkin.

Writing – original draft: Alyse A. Larkin.

Writing – review & editing: Alyse A. Larkin, Allison R. Moreno, Adam C. Martiny.

References

1. Polovina JJ, Dunne JP, Woodworth PA, Howell EA. Projected expansion of the subtropical biome and contraction of the temperate and equatorial upwelling biomes in the North Pacific under global warming. *ICES Journal of Marine Science*. 2011; 68(6):986–95.
2. Moore JK, Lindsay K, Doney SC, Long MC, Misumi K. Marine Ecosystem Dynamics and Biogeochemical Cycling in the Community Earth System Model CESM1(BGC): Comparison of the 1990s with the 2090s under the RCP4.5 and RCP8.5 Scenarios. *Journal of Climate*. 2013; 26(23):9291–312.
3. Fuhrman JA, Hewson I, Schwalbach MS, Steele JA, Brown MV, Naeem S. Annually reoccurring bacterial communities are predictable from ocean conditions. *Proceedings of the National Academy of Sciences of the United States of America*. 2006; 103(35):13104–9. <https://doi.org/10.1073/pnas.0602399103> PMID: 16938845
4. Gilbert JA, Steele JA, Caporaso JG, Steinbrueck L, Reeder J, Temperton B, et al. Defining seasonal marine microbial community dynamics. *ISME Journal*. 2012; 6(2):298–308. <https://doi.org/10.1038/ismej.2011.107> PMID: 21850055
5. Martiny AC, Talarmin A, Mouginit C, Lee JA, Huang JS, Gellene AG, et al. Biogeochemical interactions control a temporal succession in the elemental composition of marine communities. *Limnology and Oceanography*. 2016; 61(2):531–42.
6. Ward CS, Yung CM, Davis KM, Blinebry SK, Williams TC, Johnson ZI, et al. Annual community patterns are driven by seasonal switching between closely related marine bacteria. *ISME Journal*. 2017; 11(11):1412–22.

7. Hatosy SM, Martiny JBH, Sachdeva R, Steele J, Fuhrman JA, Martiny AC. Beta diversity of marine bacteria depends on temporal scale. *Ecology*. 2013; 94(9):1898–904. <https://doi.org/10.1890/12-2125.1> PMID: 24279260
8. Cram JA, Chow CET, Sachdeva R, Needham DM, Parada AE, Steele JA, et al. Seasonal and interannual variability of the marine bacterioplankton community throughout the water column over ten years. *ISME Journal*. 2015; 9(3):563–80. <https://doi.org/10.1038/ismej.2014.153> PMID: 25203836
9. McMahon KW, McCarthy MD, Sherwood OA, Larsen T, Guilderson TP. Millennial-scale plankton regime shifts in the subtropical North Pacific Ocean. *Science*. 2015; 350(6267):1530–3. <https://doi.org/10.1126/science.aaa9942> PMID: 26612834
10. Stark C, Condrón LM, Stewart A, Di HJ, O'Callaghan M. Influence of organic and mineral amendments on microbial soil properties and processes. *Applied Soil Ecology*. 2007; 35(1):79–93.
11. Jones SE, Chiu CY, Kratz TK, Wu JT, Shade A, McMahon KD. Typhoons initiate predictable change in aquatic bacterial communities. *Limnology and Oceanography*. 2008; 53(4):1319–26.
12. Shade A, Read JS, Youngblut ND, Fierer N, Knight R, Kratz TK, et al. Lake microbial communities are resilient after a whole-ecosystem disturbance. *ISME Journal*. 2012; 6(12):2153–67. <https://doi.org/10.1038/ismej.2012.56> PMID: 22739495
13. El-Swaiss H, Dunn KA, Bielawski JP, Li WK, Walsh DA. Seasonal assemblages and short-lived blooms in coastal north-west Atlantic Ocean bacterioplankton. *Environmental Microbiology*. 2015; 17(10):3642–61. <https://doi.org/10.1111/1462-2920.12629> PMID: 25244530
14. von Scheibner M, Dorge P, Biermann A, Sommer U, Hoppe HG, Jurgens K. Impact of warming on phyto-bacterioplankton coupling and bacterial community composition in experimental mesocosms. *Environmental Microbiology*. 2014; 16(3):718–33. <https://doi.org/10.1111/1462-2920.12195> PMID: 23869806
15. Wang X, Liu LL, Piao SL, Janssens IA, Tang JW, Liu WX, et al. Soil respiration under climate warming: differential response of heterotrophic and autotrophic respiration. *Global Change Biology*. 2014; 20(10):3229–37. <https://doi.org/10.1111/gcb.12620> PMID: 24771521
16. Martinez E, Antoine D, D'Ortenzio F, Gentili B. Climate-Driven Basin-Scale Decadal Oscillations of Oceanic Phytoplankton. *Science*. 2009; 326(5957):1253–6. <https://doi.org/10.1126/science.1177012> PMID: 19965473
17. Edwards M, Beaugrand G, Helaouet P, Alheit J, Coombs S. Marine Ecosystem Response to the Atlantic Multidecadal Oscillation. *Plos One*. 2013; 8(2):e57212. <https://doi.org/10.1371/journal.pone.0057212> PMID: 23460832
18. Racault MF, Sathyendranath S, Brewin RJW, Raitsos DE, Jackson T, Platt T. Impact of El Niño Variability on Oceanic Phytoplankton. *Frontiers in Marine Science*. 2017; 4.
19. Di Lorenzo E, Mantua N. Multi-year persistence of the 2014/15 North Pacific marine heatwave. *Nature Climate Change*. 2016; 6(11):1042–47.
20. Ohman MD. Introduction to collection of papers on the response of the southern California Current Ecosystem to the Warm Anomaly and El Niño, 2014–16. *Deep-Sea Research Part I-Oceanographic Research Papers*. 2018; 140:1–3.
21. Kelly TB, Goericke R, Kahru M, Song H, Stukel MR. CCE II: Spatial and interannual variability in export efficiency and the biological pump in an eastern boundary current upwelling system with substantial lateral advection. *Deep-Sea Research Part I-Oceanographic Research Papers*. 2018; 140:14–25.
22. Morrow RM, Ohman MD, Goericke R, Kelly TB, Stephens BM, Stukel MR. CCE V: Primary production, mesozooplankton grazing, and the biological pump in the California Current Ecosystem: Variability and response to El Niño. *Deep-Sea Research Part I-Oceanographic Research Papers*. 2018; 140:52–62.
23. Fagan AJ, Moreno AR, Martiny AC. Role of ENSO Conditions on Particulate Organic Matter Concentrations and Elemental Ratios in the Southern California Bight. *Frontiers in Marine Science*. 2019; 6:386.
24. Lilly LE, Ohman MD. CCE IV: El Niño-related zooplankton variability in the southern California Current System. *Deep-Sea Research Part I-Oceanographic Research Papers*. 2018; 140:36–51.
25. Bograd SJ, Buil MP, Di Lorenzo E, Castro CG, Schroeder ID, Goericke R, et al. Changes in source waters to the Southern California Bight. *Deep-Sea Research Part II-Topical Studies in Oceanography*. 2015; 112:42–52.
26. West NJ, Scanlan DJ. Niche-partitioning of *Prochlorococcus* populations in a stratified water column in the eastern North Atlantic Ocean. *Applied and Environmental Microbiology*. 1999; 65(6):2585–91. <https://doi.org/10.1128/AEM.65.6.2585-2591.1999> PMID: 10347047
27. Johnson ZI, Zinser ER, Coe A, McNulty NP, Woodward EMS, Chisholm SW. Niche partitioning among *Prochlorococcus* ecotypes along ocean-scale environmental gradients. *Science*. 2006; 311(5768):1737–40. <https://doi.org/10.1126/science.1118052> PMID: 16556835

28. Zwirgmaier K, Jardillier L, Ostrowski M, Mazard S, Garczarek L, Vault D, et al. Global phylogeography of marine *Synechococcus* and *Prochlorococcus* reveals a distinct partitioning of lineages among oceanic biomes. *Environmental Microbiology*. 2008; 10(1):147–61. <https://doi.org/10.1111/j.1462-2920.2007.01440.x> PMID: 17900271
29. Rusch DB, Martiny AC, Dupont CL, Halpern AL, Venter JC. Characterization of *Prochlorococcus* clades from iron-depleted oceanic regions. *Proceedings of the National Academy of Sciences of the United States of America*. 2010; 107(37):16184–9. <https://doi.org/10.1073/pnas.1009513107> PMID: 20733077
30. Larkin AA, Blinebry SK, Howes C, Chandler J, Zinser ER, Johnson ZI. Niche partitioning and biogeography of high light adapted *Prochlorococcus* across taxonomic ranks in the North Pacific. *ISME Journal* 2016; 10(7):1555–67. <https://doi.org/10.1038/ismej.2015.244> PMID: 26800235
31. Cohan FM, Koeppel AF. The origins of ecological diversity in prokaryotes. *Current Biology*. 2008; 18(21):R1024–34. <https://doi.org/10.1016/j.cub.2008.09.014> PMID: 19000803
32. Larkin AA, Garcia CA, Ingoglia KA, Garcia NS, Baer SE, Twining BS, et al. Subtle biogeochemical regimes in the Indian Ocean revealed by spatial and diel frequency of *Prochlorococcus* haplotypes. *Limnology and Oceanography*. 2020; 65:S220–S32.
33. Tai V, Palenik B. Temporal variation of *Synechococcus* clades at a coastal Pacific Ocean monitoring site. *ISME Journal*. 2009; 3(8):903–15. <https://doi.org/10.1038/ismej.2009.35> PMID: 19360028
34. Malmstrom RR, Coe A, Kettler GC, Martiny AC, Frias-Lopez J, Zinser ER, et al. Temporal dynamics of *Prochlorococcus* ecotypes in the Atlantic and Pacific oceans. *ISME Journal* 2010; 4:1252–64. <https://doi.org/10.1038/ismej.2010.60> PMID: 20463762
35. Needham DM, Chow CET, Cram JA, Sachdeva R, Parada A, Fuhrman JA. Short-term observations of marine bacterial and viral communities: patterns, connections and resilience. *ISME Journal*. 2013; 7(7):1274–85. <https://doi.org/10.1038/ismej.2013.19> PMID: 23446831
36. Nagarkar M, Countway PD, Yoo YD, Daniels E, Poulton NJ, Palenik B. Temporal dynamics of eukaryotic microbial diversity at a coastal Pacific site. *ISME Journal*. 2018; 12(9):2278–91. <https://doi.org/10.1038/s41396-018-0172-3> PMID: 29899506
37. Ahlgren NA, Perelman JN, Yeh YC, Fuhrman JA. Multi-year dynamics of fine-scale marine cyanobacterial populations are more strongly explained by phage interactions than abiotic, bottom-up factors. *Environmental Microbiology*. 2019; 21(8):2948–63. <https://doi.org/10.1111/1462-2920.14687> PMID: 31106939
38. Tai V, Burton RS, Palenik B. Temporal and spatial distributions of marine *Synechococcus* in the Southern California Bight assessed by hybridization to bead-arrays. *Marine Ecology Progress Series*. 2011; 426:133–U64.
39. Ferris MJ, Palenik B. Niche adaptation in ocean cyanobacteria. *Nature*. 1998; 396(6708):226–8.
40. Aronesty E. Comparison of sequencing utility programs. *The Open Bioinformatics Journal*. 2013; 7(1).
41. Cock PJA, Antao T, Chang JT, Chapman BA, Cox CJ, Dalke A, et al. Biopython: freely available Python tools for computational molecular biology and bioinformatics. *Bioinformatics*. 2009; 25(11):1422–3. <https://doi.org/10.1093/bioinformatics/btp163> PMID: 19304878
42. Bolyen E, Rideout JR, Dillon MR, Bokulich N, Abnet CC, Al-Ghalith GA, et al. Reproducible, interactive, scalable and extensible microbiome data science using QIIME 2. *Nature Biotechnology*. 2019; 37(8):852–7. <https://doi.org/10.1038/s41587-019-0209-9> PMID: 31341288
43. R Core Team. *R: A Language and Environment for Statistical Computing*. Vienna, Austria: R Foundation for Statistical Computing; 2019.
44. Oksanen J, Blanchet FG, Friendly M, Kindt R, Legendre P, McGlenn D, et al. *vegan: Community Ecology Package*. 2017.
45. Lundin D, Severin I, Logue JB, Ostman O, Andersson AF, Lindstrom ES. Which sequencing depth is sufficient to describe patterns in bacterial alpha- and beta-diversity? *Environmental Microbiology Rep*. 2012; 4(3):367–72.
46. Hennig C. *fpclust: Flexible Procedures for Clustering*. 2018.
47. Fox J, Weisberg S. *An R Companion to Applied Regression*. Second ed. Thousand Oaks, CA: Sage; 2011.
48. Jacox MG, Hazen EL, Zaba KD, Rudnick DL, Edwards CA, Moore AM, et al. Impacts of the 2015–2016 El Niño on the California Current System: Early assessment and comparison to past events. *Geophysical Research Letters*. 2016; 43(13):7072–80.
49. Kent AG, Baer SE, Mouginito C, Huang JS, Larkin AA, Lomas MW, et al. Parallel phylogeography of *Prochlorococcus* and *Synechococcus*. *ISME Journal*. 2018; 13(13):430–41.
50. Beisner BE, Haydon DT, Cuddington K. Alternative stable states in ecology. *Frontiers in Ecology and the Environment*. 2003; 1(7):376–82.

51. Schroder A, Persson L, De Roos AM. Direct experimental evidence for alternative stable states: a review. *Oikos*. 2005; 110(1):3–19.
52. Allison SD, Martiny JBH. Resistance, resilience, and redundancy in microbial communities. *Proceedings of the National Academy of Sciences of the United States of America*. 2008; 105:11512–9. <https://doi.org/10.1073/pnas.0801925105>
53. Shade A, Peter H, Allison SD, Baho DL, Berga M, Burgmann H, et al. Fundamentals of microbial community resistance and resilience. *Frontiers in Microbiology*. 2012;3. <https://doi.org/10.3389/fmicb.2012.00003> PMID: 22279445
54. Blodau C, Knorr KH. Experimental inflow of groundwater induces a "biogeochemical regime shift" in iron-rich and acidic sediments. *Journal of Geophysical Research-Biogeosciences*. 2006; 111(G2).
55. Bush T, Diao M, Allen RJ, Sinnige R, Muyzer G, Huisman J. Oxidic-anoxic regime shifts mediated by feedbacks between biogeochemical processes and microbial community dynamics. *Nature Communications*. 2017; 8(1):1–9. <https://doi.org/10.1038/s41467-016-0009-6>
56. Veraart AJ, Faassen EJ, Dakos V, van Nes EH, Lurling M, Scheffer M. Recovery rates reflect distance to a tipping point in a living system. *Nature*. 2012; 481(7381):357–U137.
57. Karl DM, Bidigare RR, Letelier RM. Long-term changes in plankton community structure and productivity in the North Pacific Subtropical Gyre: The domain shift hypothesis. *Deep-Sea Research Part II-Topical Studies in Oceanography*. 2001; 48(8–9):1449–70.
58. Flombaum P, Gallegos JL, Gordillo RA, Rincon J, Zabala LL, Jiao N, et al. Present and future global distributions of the marine Cyanobacteria *Prochlorococcus* and *Synechococcus*. *PNAS*. 2013; 110(24):9824–9. <https://doi.org/10.1073/pnas.1307701110> PMID: 23703908
59. Zinser ER, Johnson ZI, Coe A, Karaca E, Veneziano D, Chisholm SW. Influence of light and temperature on *Prochlorococcus* ecotype distributions in the Atlantic Ocean. *Limnology and Oceanography*. 2007; 52(5):2205–20.
60. Meinvielle M, Johnson GC. Decadal water-property trends in the California Undercurrent, with implications for ocean acidification. *Journal of Geophysical Research-Oceans*. 2013; 118(12):6687–703.
61. Hewson I, Fuhrman JA. Covariation of viral parameters with bacterial assemblage richness and diversity in the water column and sediments. *Deep-Sea Research Part I-Oceanographic Research Papers*. 2007; 54(5):811–30.
62. Martiny AC, Treseder K, Pusch G. Phylogenetic conservatism of functional traits in microorganisms. *ISME Journal* 2013; 7(4):830–8. <https://doi.org/10.1038/ismej.2012.160> PMID: 23235290
63. Amend AS, Martiny AC, Allison SD, Berlemont R, Goulden ML, Lu Y, et al. Microbial response to simulated global change is phylogenetically conserved and linked with functional potential. *ISME Journal*. 2016; 10(1):109–18. <https://doi.org/10.1038/ismej.2015.96> PMID: 26046258
64. Isobe K, Allison SD, Khalili B, Martiny AC, Martiny JBH. Phylogenetic conservation of bacterial responses to soil nitrogen addition across continents. *Nature Communications*. 2019; 10(1):1–8. <https://doi.org/10.1038/s41467-018-07882-8>
65. Chisholm SW. Phytoplankton Size. Primary Productivity and Biogeochemical Cycles in the Sea. 1992; 43:213–37.
66. Moore LR, Rocap G, Chisholm SW. Physiology and molecular phylogeny of coexisting *Prochlorococcus* ecotypes. *Nature*. 1998; 393(6684):464–7. <https://doi.org/10.1038/30965> PMID: 9624000
67. Martiny AC, Coleman ML, Chisholm SW. Phosphate acquisition genes in *Prochlorococcus* ecotypes: Evidence for genome-wide adaptation. *Proceedings of the National Academy of Sciences of the United States of America*. 2006; 103(33):12552–7. <https://doi.org/10.1073/pnas.0601301103> PMID: 16895994
68. Scanlan DJ, Ostrowski M, Mazard S, Dufresne A, Garczarek L, Hess WR, et al. Ecological genomics of marine picocyanobacteria. *Microbiology and Molecular Biology Reviews*. 2009; 73(2):249–99. <https://doi.org/10.1128/MMBR.00035-08> PMID: 19487728
69. Cram JA, Xia LC, Needham DM, Sachdeva R, Sun FZ, Fuhrman JA. Cross-depth analysis of marine bacterial networks suggests downward propagation of temporal changes. *ISME Journal*. 2015; 9(12):2573–86. <https://doi.org/10.1038/ismej.2015.76> PMID: 25989373
70. Doney SC, Ruckelshaus M, Duffy JE, Barry JP, Chan F, English CA, et al. Climate Change Impacts on Marine Ecosystems. *Annual Review of Marine Science*, Vol 4. 2012;4:11–37. <https://doi.org/10.1146/annurev-marine-041911-111611> PMID: 22457967
71. Cavicchioli R, Ripple WJ, Timmis KN, Azam F, Bakken LR, Baylis M, et al. Scientists' warning to humanity: microorganisms and climate change. *Nature Reviews Microbiology*. 2019; 17(9):569–86. <https://doi.org/10.1038/s41579-019-0222-5> PMID: 31213707